On the structural polydispersity of random copolymers adsorbed at interfaces: Comparison of surface and bulk distributions

Sergey V. Lishchuk[a], Rammile Ettelaie[b] and Tom Annable[c]

[a] Materials and Engineering Research Institute, Sheffield Hallam University, Howard Street, Sheffield S1 1WB, United Kingdom
[b] Food Colloids Group, School of Food Science and Nutrition, University of Leeds, Leeds LS2 9JT, United Kingdom
[c] Fujifilm Imaging Colorants Ltd, Blackley, Manchester, M9 8ZS, United Kingdom

ABSTRACT
Synthesis of random copolymers leads to a structurally polydispersed distribution of polymer chains, where one of the constituent monomers prefer residing on the interface, while the others have a tendency for remaining in the bulk. Previous studies have demonstrated the very strong dependence of the level of adsorption with the degree of blockiness and number of adsorbing residues of the chains. Using self-consistent field (SCF) calculations, we obtain the distribution of the adsorbed copolymers and compare this with the bulk distribution of such chains. In our study, the whole range of structurally polydisperse chains in the distribution derived for a given random copolymer, are simultaneously present and can compete with each other for adsorption. We show that the distribution of chains on the surface is grossly different to that in the bulk and is largely dominated by those rare chains at the tail end of the latter distribution.

1. Introduction

Controlling the stability of colloidal formulations remains an important consideration in many industrial applications where such dispersions are routinely utilised. In pharmaceutical and agrochemical industries, the uniform distribution of insoluble drugs or adjuvants, throughout what is essentially an aqueous based product, is only achieved by maintaining the stability of emulsion oil droplets containing the active component. In contrast, in paints, coatings and inkjet formulations the desired rheological behaviour of the product is often engineered through the formation of specific types of aggregate networks of colloidal particles [1]. Yet in other applications, often involving triggered controlled release, one designs for the emulsion system to lose stability as a result of a sudden change in a specific environmental factor (e.g. pH, salt concentration, temperature). One common everyday example of this is in food emulsions containing flavour ingredients. The droplets are designed to coalesce during the consumption in

the mouth, so as to the release the required flavour or aroma [2, 3]. Much of the ability to control the colloidal state of these industrial products owes itself to the availability and the wide spread use of correct polymeric dispersants in each application [4, 5].

The addition of polymers to a colloidal dispersion can induce a variety of interactions between the colloids [6, 7]. The best known of these is the often required steric repulsion, caused by overlap of polymer layers adsorbed onto two approaching particles. Other commonly mediated interactions are the bridging attraction, associated with the sparsely adsorbed layers, and the depletion flocculation, resulting from an excessive amount of free non-adsorbed polymer remaining in the solution. Our theoretical understanding of the origins of such forces, for dispersants with relatively well defined and simple polymer architectures, is nowadays rather well developed [8, 9]. By simple architectures we refer here to such structures as adsorbed or tethered homopolymers, diblock dispersants consisting of two different segments, each having a different affinity for the surface, and triblock type structures (the so called telechelic polymers) where anchoring groups are placed at the two ends of the chain. For such dispersants it is a relatively easy task to qualitatively predict the magnitude and nature of the polymer induced colloidal interactions.

There are many situations of practical interest where the above simplified view of the architecture of the dispersant polymers remains inadequate. An example of this is the situation encountered in food based emulsions, where the use of structurally well-defined but synthetic stabilisers is not allowed. Instead, one has to resort to using naturally occurring edible biopolymers, such as milk based proteins. Use of proteins as dispersants brings with it a significant degree of complexity to the problem [10]. Proteins contain hydrophobic, polar, positive and negatively charged amino acid residues, organised in a seemingly random manner so as to lead to a variety of block sizes along the polymer backbone. Predicting the nature of mediated colloidal interactions for such dispersants becomes a difficult task, to the extent that it is not an entirely trivial matter to even ascertain if the forces are going to be repulsive or attractive, and if so over what range of particle separation distances [11]. Other sources of complication arise from the simultaneous presence of many different species of surface active molecules in the system. This leads to phenomenon of competitive adsorption between different molecules which in turn can cause the composition of the adsorbed layers on the surface of the particles to alter as the colloidal particles approach each other [12, 13].

Competitive adsorption may also occur between molecules of a seemingly single species of dispersant, if there is a significant degree of polydispersity in composition or/and in size distribution of chains. In particular, the polydispersity in composition is encountered in random copolymers, comprised of two or more groups of monomer. Due to the ease of synthesis, the use of such copolymers, where one monomer has a strong affinity for the surface while the other prefers to remain in the solvent, is a common place in industry. The randomness leads to the presence of different block sizes on different chains. It is well established that the adsorption properties of the copolymers are strongly influenced by the degree of their blockiness. At the same bulk concentration and with all else being identical, chains having larger blocks are preferentially adsorbed. They lead to a higher degree of surface coverage when compared to their counterparts consisting of smaller blocks [14, 15].

In a random copolymer solution, where chains with a multitude of block sizes will simultaneously be present, it could be expected that the distribution of polymers adsorbed onto the surface will be significantly different to what is found in the bulk. Where the chains are in equilibrium between bulk and on the surface of particles, it

can be shown that the colloidal interactions mediated between the particles are those arising from an 'effective' homopolymer. This 'effective' homopolymer is made up of monomers with properties (i.e. interactions with surface, solvent, etc.) that reflect suitably averaged values of the same properties taken over different monomer groups of the random copolymer [16]. The important point here is that, in such circumstances, the interactions can be calculated relatively easily without any need for a knowledge of the distribution of adsorbed chains on the interface. However, this situation alters immediately if the solution is washed or the particles are moved to a new environment. This leads to a fractionation of the distribution of random copolymers, with the chains transferred on the surface of particle not representative of those initially added to the solution. A typical example of this is in inkjets, where during application of ink to paper the colour pigments are subjected to a new environment. It is of some importance to the functionality of such inks that the pigments aggregate quickly upon impact with the paper. The resulting increase in the viscosity reduces the lateral spread of ink on the paper and enhances the quality of printing resolution. In such applications, the non-typical nature of the stabilising chains on the surface of pigment can deter aggregation, if for example the criteria for engineering the effect were based on a typical distribution of polymers in bulk, rather than that which actually is on the surface.

The current work attempts to investigate the degree of fractionation and the compositional distribution of random copolymers that remain on the surface. The adsorption of the chain molecules to a solid wall can be modelled using different approaches, like density functional theory [17, 18] and molecular dynamics simulations [19]. Balazs et al. [20] using Monte Carlo simulations to model the adsorption of AB copolymers from solution onto a solid surface with A comonomer being attractive to the surface found that the structure of the adsorbed layer is sensitive not only to the amount of A present in the chain but also to the arrangement of the A units along the chain. Jhon et al. [21] studied by experimental measurements and computer simulations the effect of comonomer sequence distributions in random copolymers on adsorption on flat impenetrable surfaces and found that increasing the degree of blockiness in comonomer distribution enhances the adsorption of macromolecules dissolved in a good solvent. Kłos et al. [22] used Monte Carlo simulations to study conformational rearrangements in the surface layer of random AB-copolymer melts near a selective solid surface.

Unlike previous investigations [14, 15, 16, 23] which have focused on the adsorption affinity of polymers with different level of blockiness each studied one at a time, here we consider the whole compositional distribution simultaneously present in the bulk solution. In this way, polymers of varying composition in the ensemble will also compete with each other for adsorption. The distribution of adsorbed polymers on the surface will therefore be more accurately determined, then that simply inferred on the bases of the strength of adsorption of each component on its own. Our method for studying the problem involves the self-consistent field calculations, and in particular the Fleer-Scheutjens formulation for implementing such numerical calculations [24, 25, 26] and its extension to copolymers by Evers et al [27].

The rest of the paper is organised as follows. In Section 2 we outline the self-consistent field method which we use to model random block copolymers. In Section 3 we present the algorithm used to obtain the distribution of different block copolymer realisations. The results of our calculations are presented in Section 4. Finally, our conclusions are given in Section 5.

3

2. Self-consistent field method

We use the lattice-based self-consistent field (SCF) approach which was developed by Scheutjens and Fleer [16, 24, 25, 26, 27] and later generalised to polyelectrolytes by Böhmer *et al* [28] and Israels *et al* [29, 30] and to random block copolymers, which are monodisperse in length only and all possible sequences are taken into account, by van Lent and Scheutjens [31]. The main aspects of the theory are as follows.

The system consists of random block copolymer molecules, ions, and solvent molecules distributed between two parallel planar surfaces. The space between the surfaces is divided into layers, $z = 1, 2, \ldots, d$, and each layer is further divided into lattice cells of equal volume (we use the simple cubic lattice). The Bragg-Williams approximation of random mixing, implying that the distribution within each layer is not affected by mutual interactions, is applied within each layer, and thus all cells within each layer are equivalent. Each cell contains either a monomer belonging to a random block copolymer, an ion or a solvent molecule; so all the cells are occupied. In our model system we have four types of components: the solvent ($i = 0$), the random block copolymer ($i = 1$), and two types of oppositely charged ions ($i = 2, 3$). The random block copolymer component consists of two species types α; therefore, there are in total five species types ($\alpha = 0, \ldots, 4$) in the system.

The random block copolymers are assumed to be monodisperse in length only and all possible sequences are allowed. Each segment in polymer i has a probability $\nu_{\alpha i}$ to be an α segment, independent of its ranking number. Then the average fraction of α segments in polymer i is $\nu_{\alpha i}$. The transition coefficients $T_{\alpha\beta i}$ are defined which give the probability that in the molecules i the neighbouring segment of an α segment will be of type β, with $0 \leq T_{\alpha\beta i} \leq 1$ and $\sum_\beta T_{\alpha\beta i} = 1$. The transition coefficients obey the relations

$$\sum_\alpha \nu_{\alpha i} T_{\alpha\beta i} = \nu_{\beta i} \tag{1}$$

and

$$\nu_{\alpha i} T_{\alpha\beta i} = \nu_{\beta i} T_{\beta\alpha i}, \tag{2}$$

which is the probability of finding a bond between successive α and β monomers.

For random copolymers consisting of two types of segments, A and B, various combinations may be expressed in terms of the blockiness constant B_i which is defined as

$$B_i = T_{\mathrm{AA}i} - T_{\mathrm{BA}i}. \tag{3}$$

A value B_i equal to 1 ($T_{\mathrm{BA}i} = T_{\mathrm{AB}i} = 0$) corresponds to a mixture of two homopolymers A and B with bulk solution volume fractions $\nu_{\mathrm{A}i}\phi_i^{\mathrm{b}}$ and $\nu_{\mathrm{B}i}\phi_i^{\mathrm{b}}$, respectively. Here ϕ_i^{b} presents the bulk volume fraction of polymer chains. Similarly, $B_i = -1$ ($T_{\mathrm{AA}i} = T_{\mathrm{BB}i} = 0$) corresponds to an alternating copolymer, whereas for $B_i = 0$ the primary structure is fully random. The sequence distribution of a random copolymer with two different segments is completely determined by the parameters $\nu_{\mathrm{A}i}$ and B_i. Only for $\nu_{\mathrm{A}i} = 0.5$, B_i can be any number between -1 and 1. In general, the limits for

4

B_i at a given $\nu_{\mathrm{A}i}$, obtained from Eqs (1) and (3) and the condition $0 \leq T_{\mathrm{AB}i} \leq 1$, are

$$\max\left(-\frac{\nu_{\mathrm{A}i}}{\nu_{\mathrm{B}i}}, -\frac{\nu_{\mathrm{B}i}}{\nu_{\mathrm{A}i}}\right) \leq B_i \leq 1. \tag{4}$$

In the SCF approach, all of the species (monomers comprising the chains, ions, solvent) are subjected to the influence of a potential of mean force. This potential of mean force is determined as a derivative of the free energy with respect to the species concentration and it is defined to be zero in the homogeneous bulk solution far away from the surface. For any species of type α at distance z from the surface, the potential can be expressed by

$$\psi^\alpha(z) = \psi_{\mathrm{hc}}(z) + \psi_{\mathrm{int}}^\alpha(z) + \psi_{\mathrm{el}}^\alpha(z), \tag{5}$$

where $\psi_{\mathrm{hc}}(z)$ is a hard-core term, $\psi_{\mathrm{int}}^\alpha(z)$ is a contribution from nearest neighbour short-range interactions, and $\psi_{\mathrm{el}}^\alpha(z)$ is a long-range electrostatic contribution. The hard-core term $\psi_{\mathrm{hc}}(z)$ is the same for all types of species in layer z. It ensures that the space in each layer z is completely occupied according to

$$\sum_{\alpha=0} \phi^\alpha(z) = 1, \tag{6}$$

where $\phi^\alpha(z)$ are the volume fractions (density) of species α in layer z. The summation in Eq. (6) is taken over all the species types with $\alpha = 0$ corresponding to solvent molecules.

The second term in Eq. (5), $\psi_{\mathrm{int}}^\alpha(z)$ represents the short-range interactions and is expressed as

$$\psi_{\mathrm{int}}^\alpha(z) = \sum_{\beta=0}^{N_{\mathrm{type}}} \chi_{\alpha\beta}\left(\left\langle \phi^\beta(z)\right\rangle - \Phi^\beta\right) + (\delta_{z,1} + \delta_{z,d})\chi_{\alpha S}, \tag{7}$$

where $\chi_{\alpha\beta}$ is the Flory-Huggins interaction parameter between species of types α and β, $\chi_{\alpha S}$ is the interaction parameter between species of type α and the surface (S), $\delta_{z,1}$ and $\delta_{z,d}$ are the Kronecker symbols, which are equal to 1 if $z = 1$ and $z = d$ (the layers adjacent to the surfaces) and zero otherwise. The bulk volume fraction of species β is represented by Φ^β. The term in angular brackets in Eq. 7 is called the contact fraction and it denotes the average interaction of a monomer in layer z with species type β. The average is taken over all the nearest neighbours, which are located in the three consecutive layers $z - 1$, z, and $z + 1$. The contact fraction is given by

$$\left\langle \phi^\beta(z)\right\rangle = \lambda_{-1}\phi^\beta(z-1) + \lambda_0\phi^\beta(z) + \lambda_{+1}\phi^\beta(z+1). \tag{8}$$

The λ parameters are the fractions of neighbors in each of the adjacent layers, which are dependent on the lattice type used. For the simple cubic lattice adopted here, the number of the nearest neighbours for each cell is equal to 6; so we have $\lambda_{-1} = \lambda_{+1} = 1/6$ and $\lambda_0 = 4/6$.

Finally, the third term in Eq. (5), $\psi_{\mathrm{el}}^\alpha(z)$, responsible for the long-range electrostatic

interactions, is calculated as

$$\psi_{\text{el}}^{\alpha}(z) = q^{\alpha}\psi_{\text{el}}(z), \tag{9}$$

where q^{α} is the charge of species α and $\psi_{\text{el}}(z)$ is the electrostatic potential of mean force. Similar to the total potential of mean force, the electrostatic potential depends only on the distance from the surface and it is set to zero in the bulk solution far away from the surface, that is, $\psi_{\text{el}}^{\text{bulk}} = 0$ (i.e. defined with reference to its value in bulk solution). The electrostatic potential is related to the distribution of charge density through the Poisson equation

$$\epsilon_0\epsilon_r\nabla^2\psi_{\text{el}}(z) = -\rho(z). \tag{10}$$

Here ϵ_0 and ϵ_r are the permittivity of vacuum and the relative dielectric permittivity of solvent, ∇^2 is the Laplacian operator, and $\rho(z)$ is the space charge density at distance z from the surface. With the thickness of each layer given by a_0, the space charge density $\rho(z)$ is related to the plane charge density by $\rho(z) = \sigma(z)/a_0$, where the latter is calculated as

$$\sigma(z) = \sum_{\alpha} q^{\alpha}\phi^{\alpha}(z). \tag{11}$$

Equation (10) is solved with the boundary conditions $\nabla\psi = 0$ at the surfaces of the plates and at mid-point in the gap between them. The former assumes that the plates have no inherent charge of their own, distinct from that due to the adsorption of the polymers, whereas the second reflects the symmetrical nature of the problem. From now on the electrostatic potential of mean force $\psi_{\text{el}}(z)$ in Eq. (10) will be expressed in units of k_BT/e and the plane charge density $\sigma(z)$ in the units of e/a_0^2.

As is clearly seen from the set of equations above, to obtain the potentials of mean force $\psi^{\alpha}(z)$ (also called the mean fields), we need to know the density distributions $\phi^{\alpha}(z)$ for all the species types in each layer. As will be shown later, the density profiles $\phi^{\alpha}(z)$ depend in turn on the as yet unknown mean fields $\psi^{\alpha}(z)$. To obtain both sets of quantities, mean fields and volume fractions, the equations for them are solved self-consistently by an iterative procedure. As a starting point of the iteration, one of the distributions, $\psi^{\alpha}(z)$ or $\phi^{\alpha}(z)$ is initially chosen (guessed). It is convenient to start from the initial guess of the potentials or from a Boltzmann weighting factor for a single monomer

$$G^{\alpha}(z) = \exp(-\psi^{\alpha}(z)). \tag{12}$$

The quantity $G^{\alpha}(z)$ gives the probability of finding a monomer of type α in layer z relative to the probability of finding it at a point far away from the surface (the potential $\psi^{\alpha}(z)$ here is in units of k_BT). Thus, volume fractions of species consisting of single monomers, such as ions or solvent molecules, follow directly from

$$\phi_i(z) = \Phi_i G_i(z), \tag{13}$$

where the index i means the component number, as mentioned above.

For a component consisting of more than one monomer, like a polymer, we should calculate the segment distribution functions $G_i(s,z)$. The segment distribution func-

tions, $G_i(s, z)$, give the probability that a chain made up of the first s monomers of the polymer i, will end in layer z. It can be expressed through the probabilities of the $(s-1)$-mer chain via the following recurrence relation [16]:

$$G_i(s, z) = G_{t_i(s)}(z) \cdot \langle G_i(s-1, z) \rangle . \tag{14}$$

Here

$$\langle G_i(s, z) \rangle = \lambda_{-1} G_i(s, z-1) + \lambda_0 G_i(s, z) + \lambda_{+1} G_i(s, z+1), \tag{15}$$

the index $t_i(s)$ is the type (α) of the sth monomer of polymer i and the starting point is the first monomer, that is, $s = 1$ and $G_i(1, z) = G_{t_i(1)}(z)$. We also need to calculate the 'opposite' segment distribution function for each segment of polymer i, where the counting of monomer is backward, $s = N_i, N_i - 1, \dots, 1$, this is necessary for polymers with a non-symmetrical primary sequence along their backbone:

$$G_i^*(s, z) = G_{t_i(s)}(z) \cdot \langle G_i^*(s+1, z) \rangle . \tag{16}$$

The initial conditions to start the above recurrence now become $s = N_i$ and $G_i^*(N_i, z) = G_{t_i(N_i)}(z)$.

In the case of copolymers consisting of two types of segments, A and B, four transition factors can be defined: T_{AAi}, T_{ABi}, T_{BAi}, and T_{BBi}. Taking the product of transition factors into account for the calculation of the end segment distribution function, eq (14) yields

$$G_{\alpha i}(s, z) = G_{t_i(s)}(z) \cdot \sum_\beta T_{\alpha\beta i} \langle G_{\beta i}(s-1, z) \rangle . \tag{17}$$

Eq (16) becomes

$$G_{\alpha i}^*(s, z) = G_{t_i(s)}(z) \cdot \sum_\beta T_{\alpha\beta i} \langle G_{\beta i}^*(s+1, z) \rangle . \tag{18}$$

Then

$$G_i(s, z) = \sum_\alpha G_{\alpha i}(s, z) \tag{19}$$

and

$$G_i^*(s, z) = \sum_\alpha G_{\alpha i}^*(s, z) \tag{20}$$

The knowledge of all the end-point distributions from $s = 1$ to N_i for $G_{\alpha i}$ and from N_i to 1 for $G_{\alpha i}^*$ allows the volume fraction profiles for all the monomers belonging to polymer i to be determined. This is done with the aid of the composition law [16, 27]. Monomer s joins the chain parts $1, 2, \dots, s$ and $s, s+1, \dots, N_i$. For monomer s in layer z, the first chain part has a statistical weight $G_i(z, s)$ and the other a weight $G_i(z, N_i - s + 1)$ (for example, if $N_i = 10$ and $s = 3$, the monomer s will be third if

counting onward $G_i(3, z)$ and eighth if counting backward $G_i^*(8, z)$). Hence, the volume fraction of species of type α belonging to polymer i in layer z becomes

$$\phi_i^\alpha(z) = \frac{\Phi_i^\alpha}{N_i} \sum_{s=1}^{N_i} \frac{G_i(s, z)G_i^*(N_i - s + 1, z)\delta_{\alpha, t_i(s)}}{G_{t_i(s)}(z)}, \tag{21}$$

where $\delta_{\alpha, t_i(s)}$ is the Kronecker symbol, which is equal to 1 if $\alpha = t_i(s)$ and 0 otherwise, and Φ_i^α is the bulk volume fraction of the monomer species type α belonging to polymer i. The factor $G_{t_i(s)}(z)$ in the denominator arises to correct the double counting of the weighting factor of monomer s. For random block copolymers substituting Eqs (19) and (20) into Eq. (21) gives the volume fractions due to segment α:

$$\phi_i^\alpha(z) = \frac{\Phi_i^\alpha}{N_i} \sum_{s=1}^{N_i} \frac{G_{\alpha i}(s, z)G_{\alpha i}^*(N_i - s + 1, z)}{G_{t_i(s)}(z)}. \tag{22}$$

Now to obtain the potentials $\psi_\alpha(z)$ and the concentration profiles $\phi_\alpha(z)$, the set of Eqs (5–7,9,12,22) should be solved self-consistently, taking into account that the electrostatic potential $\psi_{\text{el}}(z)$ has to fulfil the Poisson equation (10). The iterations are allowed to run until the convergence is obtained with a required accuracy. The final solution obtained in this way for fields and volume fractions will satisfy the minimum for the free energy expression [15, 28]

$$
\begin{aligned}
A(r) &= \sum_i \sum_\alpha \left\{ -\sum_{z=0}^d \frac{1}{N_i} [\phi_i^\alpha(z) - \Phi_i^\alpha] - \sum_{z=0}^d \phi_i^\alpha(z)\psi_\alpha(z) \right\} \\
&+ \sum_i \sum_\alpha \chi_\alpha S [\phi_i^\alpha(0) - \phi_i^\alpha(r)] \\
&+ \frac{1}{2} \sum_{ij} \sum_{\alpha\beta} \sum_{z=0}^d \chi_{\alpha\beta} [\phi_i^\alpha(z) - \Phi_i^\alpha] \left[\phi_i^\beta(z) - \Phi_i^\beta \right] \\
&+ \frac{1}{2} \sum_{z=0}^d \sigma(z)\psi_{\text{el}}(z).
\end{aligned} \tag{23}
$$

Here $A(r)$ is the free energy in units of $k_B T$ per monomer area $\left(a_0^2\right)$ at separation r between the surfaces. The summation goes over all the components i (protein, ions, solvent) and all the monomer species types α belonging to the component i, where N_i is the number of monomers for each component i.

3. Distribution of the adsorbed polymers

Random block copolymer consists of different molecules, corresponding to particular realisations of monomer sequences. Generally, spatial distribution of each realisation does not necessarily coincide with that of the averaged spatial distribution of the random block copolymer. In particular, polymer molecules with different monomer sequences adsorb differently to the surfaces, as described in Introduction. To quantify

this difference, we need to calculate the surface excess amount of the adsorbed polymer,

$$\Gamma^{\text{ex}} = \int_0^\infty \left[\phi(z) - \phi^{\text{bulk}} \right] dz, \tag{24}$$

for each possible monomer sequence $X_1 X_2 \ldots X_N$ taken with an appropriate weight corresponding to the probability of this sequence in the random copolymer with given composition and blockiness, given by the expression

$$P_i(X_1 X_2 \ldots X_N) = \nu_{X_1} \prod_{s=2}^{N_i} T_{X_{s-1} X_s i}. \tag{25}$$

The Green functions (22) calculated by solving self-consistent field equations for a random block copolymer already contain the information needed to calculate necessary information for each particular realisation of the monomer sequence. By doing this for all possible realisations we can obtain various statistical distributions, in particular, the distribution of the excess amount of the adsorbed polymer (24) as a function of a fraction of a particular monomer type.

The total number of realisations is $N!$. This number can be reduced by taking into account that due to the symmetry condition (2) the sequence probability (25) equals

$$P_i(X_1 X_2 \ldots X_N) = P_i(X_N X_{N-1} \ldots X_1) = \nu_{X_N} \prod_{s=1}^{N_i-1} T_{X_{s+1} X_s i}. \tag{26}$$

4. Results

This Section presents the numerical results obtained using the methodology described above. First, we describe the basis configuration of the system. We use dimensionless values of the parameters.

We consider a 'water' solution of a fully dissociated 'salt' of concentration $\phi_{ion} = 0.001$. This value of the volume fraction of ions translates approximately to an ionic concentration of 0.01 mol/L, assuming the ions are Na^+ and Cl^- and roughly have the same size. This concentration is not untypical of values encountered in many applications such as foods, inkjets, or coatings.

The solution contains the fraction $\phi = 0.1$ of the random block copolymer. This value of the volume fraction of dispersants is somewhat higher than that which is normally used in practice, but was used here to ensure the saturation coverage of the surfaces by the polymer. The random block copolymer consists of two types of monomers which we denote A and B. The sequence of the monomers corresponds to zero blockiness (fully random). The monomers A and B interact with the strength described by the Flory-Huggins parameter $\chi_{AB} = 1$. Additionally we assume that the monomers of type A also interact with the solvent with the strength described by the Flory-Huggins parameter $\chi_{wA} = 1$. We also assume that the monomers of type A are uncharged while the monomers of type B bear a charge $q_B = -0.1$.

The solution is placed between two flat surfaces. The monomers of type A attract to one of the surfaces with strength $\chi_{sA} = -0.1$, while the other surface is neutral with respect to the polymer.
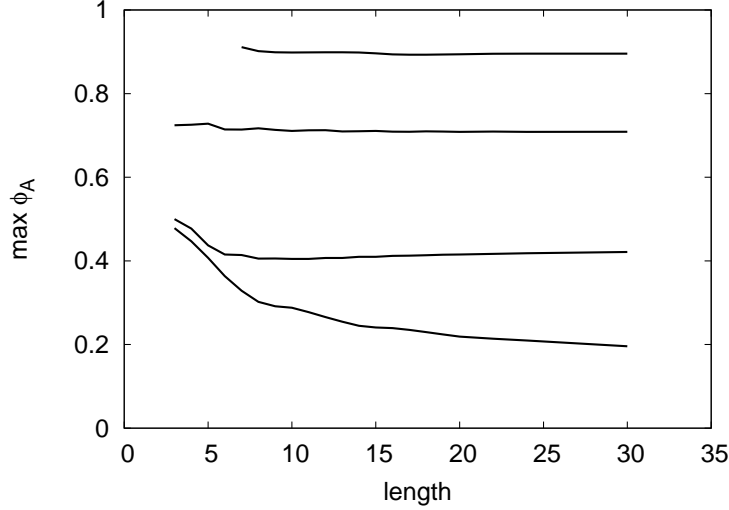
Figure 1. The fraction of A monomers at which the maximum adsorption occurs in a structurally polydisperse random copolymer of average $\langle \phi_A \rangle = 0.1$, plotted as function of length of the chains. Different curves correspond to the surface affinity values $\chi_s = -0.5, -1.0, -1.5, -2.0$ (bottom to top).

The configuration described above corresponds to the 'default' setup used in our numerical calculations. This means that the values of all the parameters are fixed as described above, except the parameters explicitly indicated to be changing.

The polymers are assumed monodisperse in length. Many properties of the polymer solutions depend on the polymerization degree N both quantitatively and qualitatively. However, the composition distribution of the adsorbed polymers, which we study here, demonstrates only week dependence if N is large enough. However, since the computation time rises combinatorially with the polymerization degree, it is necessary to choose the value of N small enough to remain within realistic computation time. Having modelled a system with different values of N (the results are shown in Figure 1), we have chosen the value $N = 20$ which we use henceforward.

First we present the results on the adsorption of fully random block copolymer, in which the blockiness $B_i = 0$. Figure 2 demonstrates that the distribution of the adsorbed polymers in ϕ_A is very different from the distribution in the bulk solution. The maximum of the distribution shifts towards larger values of ϕ_A. This shift becomes larger as the value of the surface affinity χ_s increases.

We have investigated the dependence of polymer distribution in this system upon the values of the Flory-Huggins parameter, the electrolyte concentration and the charge density and found that for the realistic values of these quantities the distribution hardly changes. As an example, the dependence of the position of the distribution maximum upon the value of the Flory-Huggins parameter χ is depicted in figure 3. With account of this, we shall henceforth use the values of these parameters given in the beginning of the present Section.

In order to investigate the dependence of the compositional distribution upon the level of blockinness, we have carried out the numerical calculations of the system at different values of the blockiness parameter B_i. The results, presented in Figure 4 and Figure 5, demonstrate that the increase in surface affinity and average block sizes mostly favour the shift of the distribution towards larger values of ϕ_A.
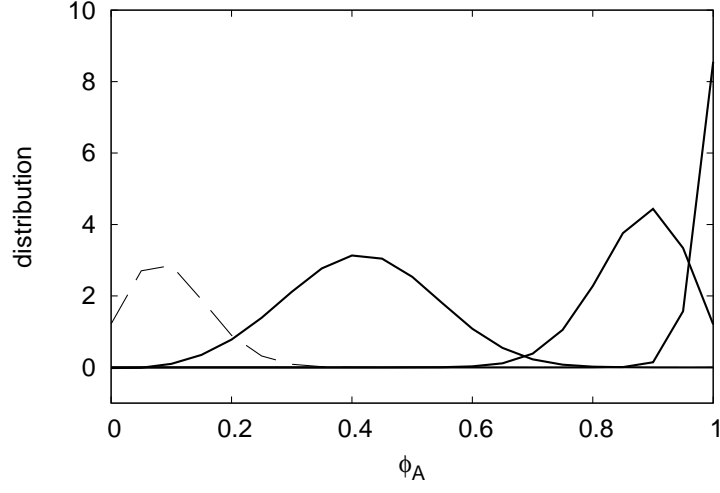
10

Figure 2. Distribution of the adsorbed polymers in ϕ_A for surface affinity values $\chi_s = -1.0, -2.0, -3.0$ (solid lines, left to right). Dashed line corresponds to the distribution in the bulk solution.
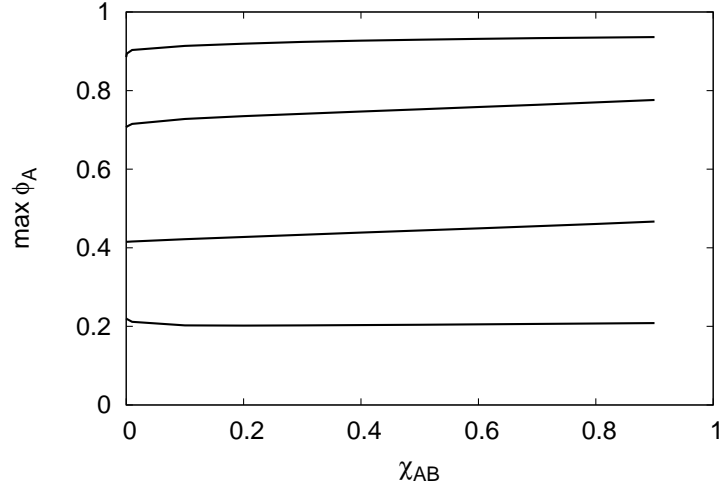

Figure 3. Position of the distribution maximum as a function of Flory-Huggins parameter χ_{AB} at surface affinity values $\chi_s = -0.5, -1.0, -1.5, -2.0$ (bottom to top).
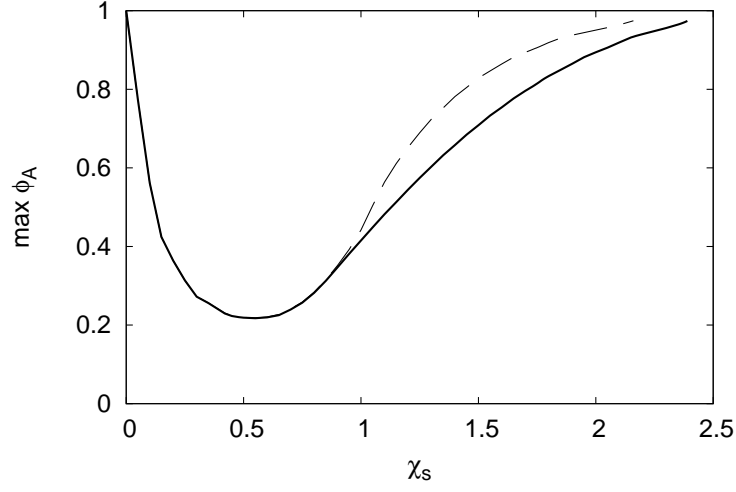
11

Figure 4. The value of ϕ_A, fraction of A monomers, at which the maximum adsorption on surface occurs for a fully random block copolymer (solid line) and for a block copolymer with blockiness value $B_i = 0.5$ (dashed line), both with $\langle \phi_A \rangle = 0.1$. Results show the change in the position of maximum with the surface affinity χ_s.
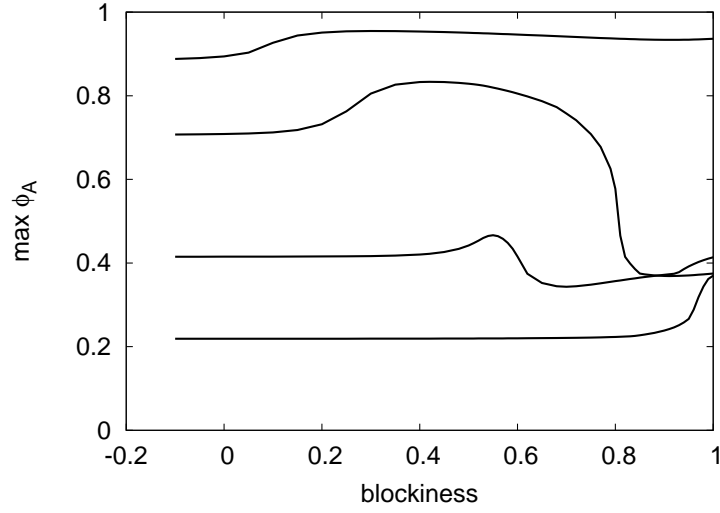

Figure 5. Position of the distribution maximum as a function of the blockiness parameter B_i. Different curves correspond to the surface affinity values $\chi_s = -0.5, -1.0, -1.5, -2.0$ (bottom to top).

12

Figure 6. Excess amount of the adsorbed polymer as a function of blockiness parameter B_i. Different curves correspond to the surface affinity values $\chi_s = -0.5, -1.0, -1.5, -2.0$ (bottom to top).
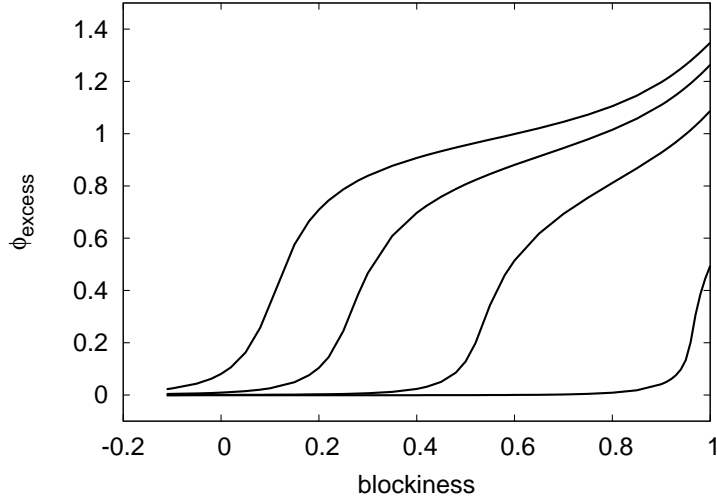
The increase in the level of blockiness also results in the increase in the excess amount of the adsorbed polymer, as demonstrated in Figure 6. This qualitatively agrees with the experimental results by Jhon et al. [21].

5. Conclusion

We have used the self-consistent field approach to model the adsorption of structurally random block copolymer molecules from a solution onto a selective solid surface. In our study, the whole range of structurally polydisperse chains in the distribution derived for a given random copolymer, are simultaneously present and can compete with each other for adsorption.

We have found that the surface compositional distribution of block copolymer molecules is very different from the corresponding distribution in the bulk and is largely dominated by those rare chains at the tail end of the latter distribution. This difference in the distribution depends upon the surface affinity as well as upon the degree of blockiness.

Our numerical SCF computations have the advantage that the full range of possible structural polydispersity can be accounted for in such calculation and involving the appropriate distribution for any given random co-polymers. The difficulty in performing simulations for such system arises from the fact that the surface adsorption is dominated by quite rare chains at the tail end of the distribution. Thus, to have a sufficient number of these to obtain a meaningful result from simulations such as Monte-Carlo or molecular dynamics, one requires to include a huge number of total chains in the system, which is difficult and time consuming even with quite advanced computer resources. Nonetheless a Monte-Carlo simulation study, has been reported by Jhon et al. [21], which involved a somewhat approximate distribution of co-polymers consisting of different sized regularly arranged blocks. Obviously, being a simulation, the numbers of different chain types included is somewhat limited. Nonetheless, it was reported

13

that polymers with larger blocks in the mixture tend to dominate at the surface. This is very much what we also find in our work.

With regards to experiments, the development of the techniqes to measure either directly or indirectly the distribution of the adsorbed random block copolymers can possibly validate our results as well as provide further insight in this problem. For example, one possible technique is to stabilise emulsions with such random co-polymers (assuming that these are amphiphilic). Then by centrifuging to separate the droplets and using a surfactant (e.g. SDS) to break up the emulsion, one can separate and examine those chains that were adsorbed at the interface. At the very least, the composition of co-polymers on the surface can easily be determined and compared to that in the bulk.

References

[1] T.F. Tadros, *Colloids in Paints*, *Colloids and Interface Science Series*, Vol. 6 (WILEY-VCH Verlag GmbH & Co. KGaA, Weinheim, 2010).

[2] E. Dickinson, *An Introduction to Food Colloids* (Oxford University Press, Oxford, 1992).

[3] P. Walstra, *Physical Chemistry of Foods* (Marcel Dekker, New York, 2003).

[4] S.V. Kuchibhatla, A.S. Karakoti and S. Seal, J. Minerals **57** (12), 52–56 (2005).

[5] E. Amstad, M. Textor and E. Reimhult, Nanoscale **3**, 2819–2843 (2011).

[6] W.B. Russel, D.A. Saville and W.R. Schowalter, *Colloidal Dispersions* (Cambridge University Press, Cambridge, 1989).

[7] R.J. Hunter, *Foundation of Colloid Science*, Vol. 1 (Clarendon press, Oxford, 1987).

[8] S. Asakura and F. Oosawa, J. Chem. Phys. **22** (7), 1255 (1954).

[9] S.T. Milner and T.A. Witten, Macromolecules **25** (10), 5495–5503 (1992).

[10] E. Dickinson, Coll. Surf. B **15**, 161–176 (1999).

[11] R. Ettelaie, N. Khandelwal and R. Wilkinson, Food Hydrocolloids **34**, 236–246 (2014).

[12] L.A. Pugnaloni, E. Dickinson, R. Ettelaie, A.R. Mackie and P.J. Wilde, Adv. Coll. Int. Sci. **107** (1), 27–49 (2004).

[13] R. Ettelaie, E. Dickinson and L. Pugnaloni, J. Phys.: Cond. Mat. **26** (46), 464109 (2014).

[14] C.M. Wijmans, F.A. Leermakers and G.J. Fleer, J. Coll. Int. Sci. **167** (1), 124–134 (1994).

[15] R. Ettelaie, B.S. Murray and E.L. James, Coll. Surf. B **31** (1-4), 195–206 (2003).

[16] G.J. Fleer, M.A. Cohen Stuart, J.M.H.M. Scheutjens, T. Cosgrove and B. Vincent, *Polymers at Interfaces* (Chapman and Hall, London, 1993).

[17] R. Tscheliessnig, W. Billes, J. Fischer, S. Sokolowski and O. Pizio, J. Chem. Phys. **124** (16), 164703 (2006).

[18] K. Bucior, J. Fischer, A. Patrykiejew, R. Tscheliessnig and S. Sokolowski, J. Chem. Phys. **126** (9), 094704 (2007).

[19] W. Billes, F. Bazant-Hegemark, M. Mecke, M. Wendland and J. Fischer, Langmuir **19** (26), 10862–10868 (2003).

[20] A.C. Balazs, M. Gempe and C.W. Lantman, Macromolecules **24**, 168–176 (1991).

[21] Y.K. Jhon, J.J. Semler, J. Genzer, M. Beevers, O.A. Guskova, P.G. Khalatur and A.R. Khokhlov, J. Chem. Phys. **42**, 2843–2853 (2009).

[22] J.S. Kłos, D. Romeis and J.U. Sommer, J. Chem. Phys. **132** (2), 024907 (2010).

[23] S. Bhattacharya, H.P. Hsu, A. Milchev, V.G. Rostiashvili and T.A. Vilgis, Macromolecules **41** (8), 2920–2930 (2008).

[24] J.M.H.M. Scheutjens and G.J. Fleer, J. Phys. Chem. **83** (12), 1619–1635 (1979).

[25] J.M.H.M. Scheutjens and G.J. Fleer, J. Phys. Chem. **84** (2), 178–190 (1980).

[26] J.M.H.M. Scheutjens and G.J. Fleer, Macromolecules **18** (10), 1882–1900 (1985).

[27] O.A. Evers, J.M.H.M. Scheutjens and G.J. Fleer, Macromolecules **23** (25), 5221–5233 (1990).

[28] M.R. Böhmer, O.A. Evers and J.M.H.M. Scheutjens, Macromolecules **23** (8), 2288–2301 (1990).

[29] R. Israels, J.M.H.M. Scheutjens and G.J. Fleer, Macromolecules **26** (20), 5405–5413 (1993).

[30] R. Israels, F.A.M. Leermarkers and G.J. Fleer, Macromolecules **27** (11), 3087–3093 (1994).

[31] B. van Lent and J.M.H.M. Scheutjens, J. Phys. Chem. **94**, 5033–5040 (1990).